MicroRNA-122a aggravates intestinal ischaemia/reperfusion injury by promoting pyroptosis via targeting EGFR-NLRP3 signaling pathway

Fei Wang
Dalian Medical University
Lidan Gu
Dalian Medical University
Yilin Wang
Affiliated Zhongshan Hospital of Dalian University
Deen Sun
Dalian Medical University
Yuanhang Zhao
Dalian Medical University
Qiang Meng
Dalian Medical University
Lianhong Yin
Dalian Medical University
Lina Xu
Dalian Medical University
Xiaolong Lu
Dalian Medical University
Jinyong Peng
Dalian Medical University
Yuan Lin
Dalian Medical University
Pengyuan Sun (pysun@dmu.edu.cn)
Dalian Medical University

Research Article

Keywords: Intestinal I/R injury, MicroRNA-122a, EGFR, Pyroptosis

Posted Date: May 4th, 2022

DOI: https://doi.org/10.21203/rs.3.rs-1600973/v1

Abstract

Multiple studies have confirmed the significance of microRNA (miR)-122a in disease regulation. However, its impact on ischaemia/reperfusion (I/R) injury is unknown. Therefore, in order to uncover new pharmacological targets for treating this condition, the regulation of intestinal I/R injury by miR-122a became the focus of this study. Two models, including hypoxia/reoxygenation (H/R)-injured IEC-6 cells *in vitro* and ischemia/reperfusion (I/R)-injured C57BL/6 mice intestinal tissues *in vivo*, were used in this study. Applying dual-luciferase reporter assays and transfection tests, the regulatory impacts of miR-122a were examined by promoting pyroptosis on intestinal I/R injury *via* targeting epidermal growth factor receptor (EGFR)- NOD-, LRR-, and pyrin domain-containing 3 (NLRP3) signaling pathway. Both H/R-injured IEC-6 cells and I/R-injured mice intestinal tissues had elevated miR-122a expression, which targeted EGFR directly. Increased miR-122a expression significantly inhibited EGFR activity, decreased EGFR mRNA and protein expression, increased NLRP3 mRNA and protein expression, and up-regulated caspase 1, N-GSDMD, ASC, IL-1β, and IL-18 protein expression to promote pyroptosis. Furthermore, in IEC-6 cells, a miR-122a inhibitor and an EGFR-overexpression plasmid significantly reduced pyroptosis, alleviating intestinal I/R injury *via* activating the EGFR-NLRP3 signaling pathway. miR-122a is very essential for regulating intestinal I/R injury. It promotes pyroptosis by blocking the EGFR-NLRP3 signaling pathway, which should be evaluated as a therapeutic target for this disease.

1. Introduction

In clinic, intestinal ischemia/reperfusion (I/R) injury can be caused by a variety of trauma or surgery, such as arterial embolism, strangulated hernia (Eryilmaz, Turkyilmaz et al. 2020), mesenteric ischemia shock (Reifegerste, Czerwinski et al. 2019), hemorrhagic shock (Zhang, Wu et al. 2020), and organ transplantation (Shen, Zhang et al. 2013, Fernandez, Sanchez-Tarjuelo et al. 2020), and severe cases can threaten the patient's life (Deitch 1992, Kip, Grootjans et al. 2021). Intestinal I/R injury includes mucosal barrier damage and bacterial translocation (Li, Xu et al. 2017, Chen, Wang et al. 2022), and it is the main cause of systemic inflammatory response syndrome (SIRS) and multiple organ dysfunction syndromes (MODS) (Feng, Yao et al. 2017, Duranti, Vivo et al. 2018, Dai, Mao et al. 2019). As a result, it is essential to study the possible pharmaceutical targets for the therapy of intestinal I/R injury.

Pyroptosis is a recently discovered and proven form of programmed cell death that causes damage to various organs, including the intestine (Jia, Cui et al. 2020). It can induce inflammatory damage as well as cell death in extreme cases under various stress settings (Kovacs and Miao 2017). Cell swelling and a typical vesicular structure can be observed in pyroptosis due to the perforation of the membrane and the difference in osmotic pressure between the interior and exterior of the cell (Zheng, Wang et al. 2021). The occurrence of pyroptosis depends on Gasdermin (GSDMs) family proteins drilling holes on cell membranes. After that, mature interleukin-1β (IL-1β) and mature interleukin-18 (IL-18) are released, along with the other cellular content damage-associated molecular patterns (DAMPs) (Frank and Vince 2019), such as ATP (Zeng, Li et al. 2019), high mobility group box 1 (HMGB1) (Jia, Zhang et al. 2019), S100 proteins (Basiorka, McGraw et al. 2016), and interleukin-1α (IL-1α) (Aizawa, Karasawa et al. 2020). This

process is distinct from the inflammatory process of apoptosis (Nirmala and Lopus 2020, Bertheloot, Latz et al. 2021). In pyroptosis, the upstream signal complexes that recruit caspase 1 are known as inflammasomes (Stein, Kapplusch et al. 2016). A sensor molecule, such as NOD-, LRR-, and pyrin domain-containing 3 (NLRP3) (Latz, Xiao et al. 2013, Coll, Holley et al. 2018, Song, Zhao et al. 2020), which captures the information, an ASC (apoptosis-associated speck-like protein including a caspase recruitment domain) protein which acts as an adaptor, and the effect protein caspase 1 which is recruited form the inflammasome (Van Opdenbosch and Lamkanfı 2019). It has been suggested that the sensor molecule NLRP3-related pyroptosis pathway is crucial in intestinal I/R injury (Jia, Cui et al. 2020, Yang, Guo et al. 2020).

MicroRNAs (miRNAs, miRs) regulate post-transcriptional target mRNA translation by preventing protein synthesis and/or promoting degradation (Paul, Bravo Vazquez et al. 2020). Recent research has proved the involvement of miRNA in regulating intestinal I/R injury. By alleviating the recovery of autophagy flux, I/R-induced apoptosis and systemic inflammation can be inhibited *via* miR-665-3p modified by locked nucleic acid *in vivo* (Li, Wang et al. 2018). Inhibition of miR-381-3p enhances nurr1-mediated epithelial development and barrier defense of the intestine, and then reduces I/R-induced damage (Liu, Yao et al. 2018). Another study discovered that miR-378 overexpression suppresses caspase 3 activation, which may prevent mice from intestinal ischemia injury (Li, Wen et al. 2017). TLR4, TRAF6, and p-IκBα are inhibited by miR-146a, which results in reducing NF-κB p65 nuclear translocation in epithelial cells and showing protection against ischemia-induced rat intestinal injury (He, Zheng et al. 2018). PTEN/NF-κB pathway regulated by miR-682 defends mice intestine to I/R-induced damage *via* lowering oxidation, inflammation, and apoptosis (Liu, Jiang et al. 2016). I/R-induced mice intestinal injury is reduced by knocking down miR-34a-5p, which promotes SIRT1-mediated regulation of epithelial oxidation and apoptosis (Wang, Yao et al. 2016). I/R-induced mice intestinal injury is alleviated by miR-29b-3p blocking the TRAF3 signaling pathway, resulting in decreased apoptosis and inflammation (Dai, Mao et al. 2019). As a result, finding new miRNA targets that can attenuate intestinal I/R injury would help in the development of new medications.

In several investigations, miR-122a has been demonstrated to play a regulatory function in a range of disorders, notably those involving the liver and intestine. For example, inflammatory microenvironments in the periportal region of miR-122a-null mice promote local phosphatase and tensin homolog on chromosome 10 down-regulation and tumor-initiating cell expansion, resulting in hepatocellular carcinoma (HCC) (Tu, You et al. 2018), and during the progression of HCC caused by the hepatitis C virus, serum miR-122a might be used as a non-invasive biomarker (El-Ahwany, Mourad et al. 2019). Furthermore, miR-122a is downregulated in cell lines of gastrointestinal cancer and in the tissues where the cancer started. miR-122a increases intestinal epithelial permeability *via* targeting epidermal growth factor receptor (EGFR) in miR-122a-TG mice and clinical samples (Zhang, Tian et al. 2017). Inhibition of miR-122a changes the interference of adenomatous polyposis coli (APC, a tumor suppressor gene) on the growth of gastrointestinal cancer cells, proving the importance of miR-122a in tumor pathogenesis (Wang, Lam et al. 2009). While TNF-α controls intestinal permeability *in vivo* and *in vitro* by causing

occludin mRNA to be degraded by miR-122a (Ye, Guo et al. 2011). However, no research has been done on the effect of miR-122a on I/R injury.

EGFR is also known as ErbB1 and HER1 (Wang 2017). It is a transmembrane glycoprotein of type I on cell surface (Itai, Yamada et al. 2017) and activated by its particular ligands, which include EGF and TGF-α (Merlino 1990). EGFR signal is crucial in controlling cell proliferation, survival, and differentiation (Ayuso-Sacido, Moliterno et al. 2010, Wang, Li et al. 2021). According to studies, exosomes targeting EGFR send antitumor microRNAs to breast cancer cells *via* systemic injection (Ohno, Takanashi et al. 2013). Many other studies show that EGFR can be used as a target gene of microRNAs for positive or negative regulation on many diseases or injuries. For example, ultraviolet ray-induced corneal epithelial cell damage in mice is alleviated by inhibiting miR-129-5p expression *via* EGFR overexpression (Yang, Gong et al. 2019). EGFR pathway is regulated by miR-21 inhibition, which reduces excessive astrocyte activation in a rat optic nerve crush model (Li, Pan et al. 2018). By inhibiting EGFR, miR-374b prevents tumor cell migration and invasion in glioma cell lines (Pan, Cao et al. 2019). However, no one knows whether EGFR is involved in intestinal I/R injury. In addition, it is also unknown whether miR-122a, which targets EGFR, has any regulating effect on intestinal I/R injury.

Therefore, the purpose of this research is to figure out how miR-122a regulates intestinal I/R injury by targeting EGFR-NLRP3 signaling pathway, as well as to find potential therapeutic targets for intestinal injury.

2. Material And Methods

2.1. Animals and intestinal I/R-induced intestinal injury model

Forty male C57BL/6 mice, weighing 18–22 g (6–8 weeks of age), were supplied by the Laboratory Animal Center of Dalian Medical University (Dalian, China, permit number SYXK 2018-0007). Following the guidelines from the National Institute of Health, all animal researches were operated in a way that obeyed those guidelines. All animal trials obeyed the reduction, refinement, and replacement criteria (the 3Rs). Five groups of mice were randomly assigned (n = 8): one sham operation group and four intestinal I/R groups (ischemia 45 min, reperfusion 45, 90, 180, and 360 min). Mice were sedated with 1% sodium pentobarbital (50 mg/kg), and the abdominal cavity was opened to investigate the superior mesenteric artery (SMA). SMA was inspected and sutured in the sham operation group. The abdominal cavity was opened in the intestinal I/R group. SMA and its surrounding tissues were carefully separated, and SMA was briefly blocked for 45 min using a non-invasive vascular clamp to establish ischemia, then the clamp was gently withdrawn, and reperfusion was conducted for 45, 90, 180, and 360 min. By detecting variations in the color of tiny intestine segments, the I/R-injured model was successfully established.

2.2. Cell culture and hypoxia/reoxygenation (H/R) model

The American Type Culture Collection (ATCC) provided rat intestinal epithelial cells (IEC-6) which were cultured in Dulbecco's minimal essential medium (DMEM) (Gibco, CA, USA) supplemented with 10% fetal bovine serum (FBS) (Gibco, CA, USA) in a 37℃ incubator with 5% CO_2 and 21% O_2 (Thermo Fisher Scientific, Inc., USA). Cells were subcultured using 0.25% trypsin solution containing ethylene diamine tetraacetic acid (EDTA) (Servicebio, Wuhan, China) in all tests. To achieve hypoxia, normal IEC-6 cells were put in a 37℃ incubator with 5% CO_2, 1% O_2, and 95% N_2 for 4 h. Once the hypoxia was complete, the cells were subsequently cultured under usual circumstances for 0, 120, 720, and 1440 min to accomplish reoxygenation. Except culture condition (5% CO_2 and 21% O_2, 37℃), the positive control cells received the same therapy as the H/R group. Due to cell morphology and activity were almost identical in each control group, therefore, one control group was used as the representative result in this study. Cells from less than 8 generations were used to complete the study.

2.3. Cell viability and lactate dehydrogenase (LDH) assessments

Cell viability was tested using cell counting kit 8 (CCK-8) according to the manufacturer's instructions (Bio-Tool, Beijing, China). Cells were cultivated in an incubator (37℃) with 95% N_2 and 5% CO_2 for 4 h before being switched to 95% O_2 and 5% CO_2 for various time periods (0, 120, 720, and 1440 min). After that, each well was filled with 10 μL of CCK-8 and 90 μL of medium, and incubated for 45 min at 37℃. Optical density (OD, 450 nm) was finally measured.

Lactate dehydrogenase (LDH) is released into the circulation when LDH-containing cells are injured or sick, resulting in a rise in LDH level. After experimental methodological treatment, blood and cell culture medium were collected *in vivo* and *in vitro*, and the release of LDH was measured as OD value (450 nm) using a commercial kit (Nanjing Jiancheng, China) by microplate technique.

2.4. Histopathological examination

After reperfusion, intestinal tissue samples were collected and cut into 5 μm thick slices for histopathological damage detection and hematoxylin and eosin (H&E) staining. Blind observation and quantitative evaluation of tissue were used to assess mucosal histological damage. Small intestine injury was assessed using Chiu's scoring categorization.

2.5. Hoechst 33342/Propidium Iodide (PI) staining

Double staining, Propidium iodide (PI) and Hoechst 33342, were carried out according to the manufacturer's kits instructions (Solarbio, Beijing, China). Due to PI can not get through healthy cell membranes, it can be used to stain necrotic cells that have lost the integrity of their cell membranes, whereas Hoechst 33342 can be used for staining both normal and necrotic cells, and the necrotic cells fluorescein are stronger than normal cells after staining. About 1×10^5 to 1×10^6 cells were collected from each sample in a 1.5 mL centrifuge tube, and the supernatant was centrifuged. Cell precipitate was suspended in 0.8 to 1 mL cell staining buffer, then 5 μL Hoechst 33342 staining solution and 5 μL PI

staining solution were added, followed by mixing and incubation at 4℃ for 20 to 30 min. Finally, pictures were collected at a magnification of 200 times using a fluorescent microscope (Leica, Germany).

2.6. Enzyme-linked immunosorbent assay (ELISA)

Mice intestinal tissues were ground in precooled PBS at low temperature to homogenate, and IEC-6 cells were repeatedly freeze-thawed in precooled PBS to lysis, then both of them were centrifuged (12,000 rpm) at 4℃ for 15 min. Finally, IL-1β and IL-18 levels were detected in supernatant using ELISA kit (Lengton, Shanghai, China) according to manufacturer's instructions.

2.7. Dual-luciferase reporter assay

EGFR cDNAs with the putative (EGFR-WT) or mutant (EGFR-MUT) miR-122a binding site were generated. In 12-well plates, IEC-6 cells were co-transfected with miR-122a mimic and EGFR-WT, miR-122a mimic negative control (NC) and EGFR-WT, miR-122a mimic and EGFR-MUT, miR-122a mimic NC and EGFR-MUT, miR-122a inhibitor and EGFR-WT, miR-122a inhibitor NC and EGFR-WT, miR-122a inhibitor and EGFR-MUT, and miR-122a inhibitor NC and EGFR-MUT. After 24 h of transfection, luciferase activity was determined with Dual-luciferase reporter assay kit (Transgen Biotech, Beijing, China) (n = 5), which had been adjusted to firefly luciferase activity.

2.8. miR-122a mimic and EGFR-overexpression plasmid co-transfection assays

The experiments were separated into four groups: control, miR-122a mimic NC and EGFR-overexpression plasmid NC co-transfection, EGFR-overexpression plasmid single transfection, and miR-122a mimic and EGFR-overexpression plasmid co-transfection group. To make solution A, GP-transfect-Mate (Genepharma, Jiangsu, China) was dissolved in DMEM and left for 5 min. miR-122a mimic (or miR-122a mimic NC) and EGFR-overexpression plasmid (or EGFR-overexpression plasmid NC) were dissolved in DMEM to generate solutions B (or D) and C (or E). Following that, solution D and E were combined with solution A to form solution F. Solution G was produced by combining solution C and solution A, and solution H was produced by combining solution B and solution C. At room temperature, solutions F, G, and H were set for 20 min. IEC-6 cells were transfected for 6 h at 37℃ with solutions F, G, and H. The medium was then replaced with new media and cultivated under normal conditions. At 24 h after transfection, Quantitative real-time PCR (qPCR) assay was used to determine mRNA for EGFR. Protein for EGFR was determined by western blotting assay (n = 5).

2.9. Immunofluorescence assay

In vivo, closed with 3% BSA-PBS, the paraffin sections were kept for 1.5 h before being treated overnight at 4℃ with anti-EGFR antibody (catalogue: 18986-1-AP, 1:100, Proteintech, Wuhan, China) and anti-NLRP3 antibody (catalogue: #15101, 1:100, Cell Signaling Technology, USA) diluents. The next day, sections were incubated with fluorescein-labeled secondary antibody for 50 min, and stained with 4-6-diamino-2-phenylindole (DAPI) (1 μg/mL). *In vitro*, immunofluorescence staining was once used to identify EGFR and NLRP3 expression in IEC-6 cells. In 24 well plates, IEC-6 cells were fastened with 4%

paraformaldehyde and treated overnight with rabbit anti-EGFR antibody (catalogue: 18986-1-AP, 1:200, Proteintech, Wuhan, China) or anti-NLRP3 antibody (catalogue: #15101, 1:200, Cell Signaling Technology, USA). After that, the second goat anti-rabbit antibody (catalogue: SA00001-2, 1:2000, Proteintech, Wuhan, China) was incubated for 50 min before being stained with DAPI. A fluorescence microscope (Leica, Germany) was used to check the results, and the representative fields were chosen for checking.

2.10. Quantitative real-time PCR assay

A kit called TransZol (Transgen Biotech, Beijing, China) was used to get total RNA. Then, a kit called TransStart Top Green qPCR SuperMix (Transgen Biotech, Beijing, China) was used to reverse-transcribe the RNA into cDNA. When qPCR performed, Bio-Rad CFX96 PCR system and SYBR Green Master Mix were used. The levels of mRNA were compared to β-actin, and the $2^{-\triangle\triangle Ct}$ methodology was used to find the relative level of mRNA (n = 5). Primer sequences were listed in Supplemental Information Table S1.

2.11. Western blotting assay

Western blotting was used to determine protein expression (n = 6). In brief, RIPA lysis buffer (Servicebio, Wuhan, China) was used to get total protein, and nuclear protein was obtained with 15000g lysis for 15 min. After determining its concentration, the protein was separated using SDS-PAGE and transported to a polyvinylidene fluoride (PVDF) membrane. The resulting blots were blocked with 8% skim milk and incubated with anti-EGFR antibody (catalogue: 18986-1-AP, 1:1000, Proteintech, Wuhan, China), anti-NLRP3 antibody (catalogue: #15101, 1:1000, Cell Signaling Technology, USA), anti-caspase 1 antibody (catalogue: 22915-1-AP, 1:1000, Proteintech, Wuhan, China), anti-N-terminal Gasdermin D (GSDMD) antibody (catalogue: ab219800, 1:1000, Abcam, USA), anti-ASC antibody (catalogue: WL02462, 1:1000, Wanleibio, Shenyang, China) and anti-β-actin antibody (catalogue: CL594-66009, 1:1000, Proteintech, Wuhan, China) overnight at 4℃. Then, the blots were incubated with anti-rabbit (catalogue: SA00001-2, 1:2000, Proteintech, Wuhan, China) or anti-mouse (catalogue: SA00001-1, 1:2000, Proteintech, Wuhan, China) secondary antibody for 2 h at 37℃. The protein was then detected using an enhanced chemiluminescence (ECL) system. As a reference, protein expression was adjusted to β-actin.

2.12. Transfection of miR-122a inhibitor in vitro

GP-transfect-Mate was diluted in DMEM and balanced for 5 min. Both miR-122a inhibitor and miR-122a inhibitor NC were solved in DMEM. MiR-122a inhibitor and its NC at 50 nM were used as transfection concentration. Each solution was combined with GP-transfect-Mate transfection reagent as recommended by the manufacturer. Later, the solution was gently combined for 20 min. Then, the transfection mix was added to the cultured IEC-6 cells. The transfection medium was replaced with complete medium after 6 h, and the cells were processed after 24 to 48 h. Western blotting and immunofluorescence assays were used to determine the levels of EGFR and NLRP3 protein expression.

2.13. Transfection of EGFR-overexpressed recombinant lentivirus in vitro

IEC-6 cells in good condition were digested and suspended again. In addition, a suitable number of cells were inoculated and incubated overnight at 37℃. EGFR overexpressed recombinant lentivirus and control virus were mixed and diluted with the medium at 1:10 (total volume: about 2 mL), and then polybrene (final concentration: 5 μg/mL) was included in the mixture. The original culture medium of the 6-well plate was discarded and replaced with virus diluent, which was incubated in a 37℃ incubator. The virus dilution in the 6-well plate was removed after 24 h and replaced with 2 mL DMEM, which was also incubated at 37℃. Results were observed and recorded under green fluorescent protein (GFP) fluorescence under an inverted fluorescence microscope (Leica, Germany) at 72 h. After successful infection, IEC-6 cells were processed. EGFR and NLRP3 mRNA expression levels were determined using a qPCR assay, and their protein expression levels were determined using western blotting and immunofluorescence assays.

2.14. Materials

ShangHai Lengton Bioscience Co., Ltd. provided the detection boxes for the IL-1β and IL-18 double-antibody sandwich ELISAs (Shanghai, China). Beijing TransGen Biotech Co., Ltd. provided TransZolTM, TransScript® All-in-One First-Strand cDNA Synthesis SuperMix for qPCR (One-Step gDNA Removal), TransStart® Top Green qPCR SuperMix, and Double-Luciferase Reporter Assay Kit (Beijing, China). Wuhan Servicebio Biotechnology Co., Ltd. provided the Tissue Protein Extraction Kit and bicinchoninic acid protein test kit (Wuhan, China). Dalian Meilun Biotech Co., Ltd. provided the SDS-Polyacrylamide gel and the hydroxymethyl aminomethane (Dalian, China). Suzhou Genepharma Co., Ltd. provided the miR-122a inhibitor, miR-122a mimic, and EGFR-overexpression plasmid (Jiangsu, China). Shanghai GeneCopoeia Biotechnology Co., Ltd. provided the EGFR cDNAs (Shanghai, China). The substances utilized in the experiment were all analytical reagents.

2.15. Statistics

Data were presented as mean ± SD. The SPSS18.0 software (SPSS Inc., USA) was used to conduct all statistical analyses. GraphPad (version 7) Prism software (GraphPad Software, CA) was used to draw the figures. A two-tailed Student's t-test for independent samples was used to evaluate parametric variable comparisons between two groups. The one-way ANOVA and Tukey's post-hoc test were used to analyze comparisons between various groups. The Kruskal-Wallis test was used to determine the statistical significance of nonparametric differences. The relative protein or mRNA expression values were represented as "fold difference" by comparing them to the matching control value, and the control value was adjusted to 1.0 for western blotting and qPCR analyses. A statistically significant level was defined as $P < 0.05$.

3. Results

3.1. H/R and intestinal I/R promoted injury in vitro and in vivo

Figures 1A and 1B illustrated the effects on the activity, number, and shape of IEC-6 cells, with 120 min of reoxygenation causing the most serious injury. However, as compared to 120 min of reoxygenation, the extended reoxygenation time resulted in improved cell morphology and activity. After I/R, H&E staining revealed a considerable increase in inflammatory cell infiltration and necrosis (Fig. 1C). As observed in Figs. 1C and 1D, the effects of 45 min of ischemia and 45, 90, 180, and 360 min of reperfusion on mice intestinal tissue were detected, with 90 min of reperfusion causing the most serious injury. Based on Chiu's score and H&E staining results, the intestinal injury improved with a longer reperfusion duration compared to 90 min.

3.2. EGFR is miR-122a's target gene

As demonstrated in Fig. 2A, compared to the normal control cell or sham operation mice group, the expression level of miR-122a mRNA gradually increased after the IEC-6 cells were hypoxia for 4 h and reoxygenation for 120 min, and the mice were ischemia for 45 min and reperfusion for 90 min. The maximum levels of mRNA expression were observed at 120 min *in vitro* and 90 min *in vivo*, respectively. However, when reoxygenation duration ranged from 120 to 1440 min *in vitro* and reperfusion time spanned from 90 to 360 min *in vivo*, the mRNA expression levels of miR-122a were dramatically lowered. As illustrated in Fig. 2B, the 3'-UTR of EGFR mRNA contained the complementary location of miR-122a's seed region, as determined by RNA sequence alignment. The relative expression level of luciferase in the EGFR-WT + miR-122a mimic group was substantially lower than that in the EGFR-WT + miR-122a mimic NC group, but it was significantly higher in the EGFR-WT + miR-122a inhibitor group than that in the EGFR-WT + miR-122a inhibitor NC group (Fig. 2C). However, compared with the EGFR-MUT + miR-122a mimic NC group or the EGFR-MUT + miR-122a inhibitor NC group, no significant relative expression change of luciferase in the EGFR-MUT + miR-122a mimic group or the EGFR-MUT + miR-122a inhibitor group was found. The above results indicated that specific binding sites occurred between EGFR and miR-122a. As observe in Fig. 2D, the plasmid was EGFR-overexpression plasmid, the NCs were EGFR-overexpression plasmid NC and the miR-122a mimic NC. Furthermore, when contrasted to the control group, the mRNA expression level of EGFR was dramatically enhanced after transfection with EGFR-overexpression plasmid, showing that the EGFR-overexpression plasmid was effectively transfected into cells (Fig. 2D). Nevertheless, the EGFR mRNA level was much lower in the group co-transfected with EGFR-overexpression plasmid and miR-122a mimic than that in the group transfected with EGFR-overexpression plasmid alone, indicating that miR-122a suppressed EGFR expression (Fig. 2D). Figure 2E showed that following transfection with an EGFR-overexpression plasmid, the EGFR protein level was considerably higher than that in the control group. However, when EGFR protein expression was co-transfected with EGFR-overexpression plasmid and miR-122a mimic, the EGFR protein level was much lower than that in the EGFR-overexpression plasmid group (Fig. 2E). In brief, these findings showed that EGFR was a target gene of miR-122a.

3.3 miR-122a adjusted EGFR signal pathway

Figures 3A and 3B revealed that the levels of EGFR protein expression were considerably lower in the H/R (Fig. 3A) and I/R (Fig. 3B) groups as compared to the normal control or sham operation groups. However,

when reoxygenation or reperfusion time was extended beyond 120 min *in vitro* (Fig. 3A) or 90 min *in vivo* (Fig. 3B), the amount of EGFR protein expression increased. In contrast, NLRP3, ASC, caspase 1, and N-GSDMD protein expression levels were considerably higher in the H/R (Fig. 3A) and I/R (Fig. 3B) groups contrasted to the normal control or sham operation groups. However, NLRP3, ASC, caspase 1, and N-GSDMD protein expression levels dropped when reoxygenation or reperfusion duration was extended beyond 120 min *in vitro* (Fig. 3A) or 90 min *in vivo* (Fig. 3B). As observed in Figs. 3C and 3D, the protein levels of IL-1β (Fig. 3C) and IL-18 (Fig. 3D) were maximal at 120 min of reoxygenation *in vitro* or 90 min of reperfusion *in vivo*, and declined with further extension of reoxygenation or reperfusion duration by ELISA kit. As observed in Fig. 3E, the release of LDH increased rapidly during the reoxygenation of 0 to 120 min in IEC-6 cells, but this rapid increase was slowed down during 120 to 1440 min compared with 0 to 120 min. At 90 min of intestinal reperfusion, the release of LDH was maximal as compared to the sham operation group. After 90 min, the release of LDH exhibited a decreasing trend when reperfusion was prolonged. The above experimental results indicated that IEC-6 cell hypoxia for 4 h and reoxygenation for 120 min, and mice intestine ischemia for 45 min and reperfusion for 90 min, were appropriate times to establish experimental models, and these times were used to complete the subsequent experiments in this study.

3.4. H/R and I/R caused intestinal inflammation and EGFR-NLRP3-related pyroptosis

qPCR (Fig. 4A) and western blotting (Fig. 4B and 4C), as well as DAPI immunofluorescence staining (Fig. 4D and 4E), were used to assess EGFR and NLRP3 mRNA and protein expression levels. Results showed that the mRNA and protein expression levels of EGFR in the H/R or I/R groups were lower than those in the normal control or sham operation groups, but the mRNA and protein expression levels of NLRP3 in the H/R or I/R groups were higher than those in the normal control or sham operation groups. As discovered in Fig. 4F, the number of cell necrosis in the H/R group was significantly greater than that in the normal control group based on Hoechst 33342 and PI staining results. These results confirmed that pyroptosis occurred in such established models.

3.5. Inhibitor of miR-122a reduced H/R-induced injury in vitro

Figure 5A showed that, as compared to the normal control group, cell number, morphology, and viability did not change substantially after transfection with miR-122a inhibitor, demonstrating that miR-122a inhibitor had no adverse effects on normal cells. As observed in Figs. 5B and 5C, EGFR and NLRP3 protein expression levels were measured by western blotting and DAPI immunofluorescence staining. After transfected with miR-122a inhibitor, results indicated that EGFR expression was enhanced and NLRP3 expression was lowered when contrasted to the H/R group. Furthermore, when contrasted to the H/R group, results showed that LDH release (Fig. 5D) was reduced, and the total of cell necrosis (Fig. 5E) was lessened, checking by Hoechst 33342 and PI staining, after transfected with miR-122a inhibitor,

indicating pyroptosis reduction.Thus, miR-122a inhibitor inhibited intestinal I/R injury by increasing EGFR signaling and attenuating NLRP3 signaling.

3.6. Overexpression of EGFR minimized H/R-induced injury in vitro

As observed in Fig. 6A, as compared to the normal control group, cell number, morphology, and viability did not change significantly after transfected with EGFR-overexpression plasmid, demonstrating that EGFR-overexpression plasmid did not cause adverse effects in normal cells. Cells successfully transfected with EGFR-overexpression plasmid were observed by GFP fluorescence, and results showed that more than 70% of the IEC-6 cells were successfully transfected (Fig. 6B). As observed in Fig. 6C, EGFR and NLRP3 mRNA expression levels were determined by a qPCR assay, and results revealed that after transfected with EGFR-overexpression plasmid, EGFR expression was raised and NLRP3 expression was lowered, as contrasted to the H/R group. As observed in Figs. 6D and 6E, the protein expression levels of EGFR and NLRP3 were detected by western blotting and DAPI immunofluorescence staining, respectively. Results showed that, when contrasted to the H/R group, the protein expression level of EGFR was enhanced, while the protein expression level of NLRP3 was lessened after transfected with EGFR-overexpression plasmid. Furthermore, when contrasted to the H/R group, results showed that the release of LDH (Fig. 6F) was decreased, and the total of cell necrosis (Fig. 6G) was reduced, checking by Hoechst 33342 and PI staining, after transfected with EGFR-overexpression plasmid, indicating pyroptosis reduction. Thus, EGFR-overexpression plasmid mitigated intestinal I/R injury by increasing EGFR signaling and attenuating NLRP3 signaling.

4. Discussion

Blood flow to the target organ is reduced or completely blocked, resulting in tissue hypoxia, which is defined as ischemia (Li, Hu et al. 2016). Significant lack of blood supply to the intestine can be induced by thrombosis or obstruction of the mesenteric arteries caused by emboli related to cardiac illness (Puleo, Arvanitakis et al. 2011). Reduced blood flow interrupts the oxygen supply required for cell activity, resulting in cell damage and death (Li, Hu et al. 2016, Lillo-Moya, Rojas-Sole et al. 2021). Restoring blood flow is crucial to rescue and preserve normal cellular function. Nevertheless, ischemia promotes the creation of toxic compounds as well as the generation of inflammatory and epithelial cell apoptosis and necrosis (Gonzalez, Moeser et al. 2015, Liu, Chen et al. 2019). Pyroptosis is a type of pro-inflammatory programmed cell death that differs from apoptosis and necrosis (Shi, Gao et al. 2017, Frank and Vince 2019, Bertheloot, Latz et al. 2021). It is defined as the production of membrane pores mediated by cystease cutting Gasdermin D, resulting in membrane rupture and cell content leakage, as well as the release of a significant number of inflammatory mediators, such as IL-18, IL-1β, and others (He, Wan et al. 2015, Broz, Pelegrin et al. 2020). Multiple studies have discovered the function of pyroptosis in the incidence and development of inflammatory illnesses, immunological tumors, and other disorders (Chen, Shi et al. 2019, Wu, Lin et al. 2019, Shen, Wang et al. 2021). Pyroptosis shows its critical role in the genesis, progression, and prognosis of several digestive organ illnesses, such as hepatitis cirrhosis,

inflammatory bowel disease, and intestinal inflammation (Huang, Feng et al. 2019, Zuo, Zhou et al. 2020, Wang, Zhou et al. 2021). And in previous studies, the presence of pyroptosis in intestinal I/R injury has been demonstrated (Rathinam, Vanaja et al. 2012, He, Wan et al. 2015, Jia, Cui et al. 2020, Wang, Fan et al. 2020). In this study, we verified the presence of pyroptosis with LDH kit detection and Hoechst 33342/PI double staining. Furthermore, we detected Gasdermin D, IL-18, and IL-1β, which are indicators of pyroptosis. It was found that at both mRNA level and protein level, pyroptosis mainly increased after 45 min ischemia and 90 min reperfusion in C57BL/6 mice, while in IEC-6 cells, pyroptosis mainly increased after 4 h hypoxia and 120 min reoxygenation. Both *in vivo* and *in vitro*, the number of pyroptosis decreased with the extension of reperfusion or reoxygenation time after fixed ischemia or hypoxia time, and after reperfusion for 360 min or reoxygenation for 1440 min, the number of pyroptosis almost returned to the level of the sham operation group or control group.

miRNAs are endogenous non-coding RNA with a length of 19–22 nucleotides that are induced in the nucleus by RNA polymerase II (Lee, Ahn et al. 2003, Mendell and Olson 2012, Xue, Yang et al. 2021). These miRNAs are subsequently transported to the cytoplasm by exportin-5 and further processed into double-stranded mature miRNAs by the RNase III endonuclide Dicer (Lee, Ahn et al. 2003). It has been proposed that certain miRNAs have a pathogenic function in intestinal I/R injury. For example, by modulating miR-351-5p/MAPK13-mediated inflammation and apoptosis, dioscin reduces intestinal I/R injury in rats (Zheng, Han et al. 2019). Autophagy is inhibited by activating miRNA-182/Deptor/mTOR axis to minimize intestinal I/R injury in mice (Li, Luo et al. 2020). In addition to intestinal I/R injury, mir-122a has also been found to play a role in the regulation of other diseases. An investigation on human HCC shows cyclin G1 is a gene target of miR-122a, which is regularly down-regulated in this cell line (Gramantieri, Ferracin et al. 2007). In gastrointestinal malignancies, miR-122a performs as a new tumor suppressor downstream of APC (Wang, Lam et al. 2009). Nevertheless, the effect of miR-122a on I/R injury has yet to be documented. In this study, we investigated the potential pathogenic mechanism of miR-122a in intestinal I/R injury. Results indicated that the mRNA expression of miR-122a was considerably higher in the H/R or I/R groups compared to the normal control or sham operation groups, but reduced when reoxygenation or reperfusion time was prolonged. Furthermore, using several databases, we discovered that miR-122a had binding sites with EGFR, and the results were confirmed using the Dual-luciferase reporter assay. The protein and mRNA expression levels of EGFR were considerably higher when the EGFR-overexpression plasmid was transfected into IEC-6 alone compared to the control group in the co-transfection experiment. However, co-transfection of miR-122a mimic and EGFR-overexpression plasmid with IEC-6 led to lower expression levels of EGFR protein and mRNA than that only EGFR-overexpression plasmid was used. These results suggest that miR-122a directly targets EGFR.

Intestinal I/R injury is one of the most dangerous conditions in clinic (Kip, Grootjans et al. 2021). It is caused by hemorrhagic shock, trauma, strangulation ileus, acute mesenteric ischemia, and other pathological conditions (Matsuda, Yang et al. 2014, Shoup 2018, Qasim, Li et al. 2020). Until now, there is no established treatment for this injury in clinic. Most of the drugs discovered have been designed to reduce the complications associated with it (Li, Xu et al. 2017, Hu, Mao et al. 2018, Chen, Mohr et al.

2020, Jia, Cui et al. 2020). According to research, the most serious outcome of intestinal I/R injury is mucosal barrier failure, which can lead to SIRS, MODS, and ultimately death (Rutgeerts, Sandborn et al. 2005, Duranti, Vivo et al. 2018, Zhang, Wu et al. 2020). This work demonstrated that pyroptosis is a vital factor in the development of SIRS and MODS following intestinal I/R injury. We performed a miR-122a inhibitor transfection experiment to further investigate the regulating mechanism of miR-122a in intestinal I/R injury. Our findings revealed that miR-122a worsened pyroptosis by suppressing EGFR protein expression and then enhancing NLRP3 protein expression, consequently aggravating intestinal I/R injury. The above results indicate that the miR-122a-EGFR-NLRP3 signaling pathway may be a priority attraction for the advancement of novel medicines to treat intestinal I/R injury.

EGFR signaling pathway appears on epithelial, fibroblast, glial, keratinocyte, and other cell surfaces. Its function is involved in cell growth, proliferation, differentiation, and other physiological activities (Zhu, Shimizu et al. 2011, Sasada, Azuma et al. 2016, Purba, Saita et al. 2017). Patients with epithelial-derived cancers show high levels of EGFR expression, which suggests that EGFR might be utilized as a target for anticancer drug delivery systems (Ohno, Takanashi et al. 2013, Arkhipov, Shan et al. 2014). Another study on I/R-induced acute renal injury in mice shows that cathelicidin-related antimicrobial peptides inhibit NLRP3 inflammasome activation, which requires the participation of EGFR (Pan, Liang et al. 2020). However, no reports indicate how EGFR participates in intestinal I/R injury. As a result, we investigated the changes on EGFR expression under H/R and I/R conditions compared to normal control or sham operation groups in this research. By using qPCR, western blotting, and immunofluorescence assays, we discovered that EGFR expression was considerably lower in H/R or I/R groups contrasted to normal control or sham operation groups. However, contrasted to the H/R group, the corresponding pyroptosis indicators were ameliorated in H/R group under transfection with EGFR-overexpression plasmid condition, resulting in improvement of H/R-induced cell injury. Based on these findings, it could be suggested that EGFR plays a significant regulatory role in I/R-induced intestinal injury. However, whether EGFR can be selected as a biomarker in I/R-induced intestinal injury remains to be clarified.

This study found that miR-122a targeted EGFR-NLRP3 signaling pathway to affect intestinal I/R injury by regulating pyroptosis. We hope that this mechanism can be a beneficial therapeutic target for the identification and treatment of intestinal I/R injury in the future.

Abbreviations

APC, Adenomatous polyposis coli; ASC, Apoptosis-associated speck-like protein containing a caspase recruitment domain; CCK-8, Cell counting kit 8; DAMPs, Damage-associated molecular patterns; DAPI, 4',6-Diamidino-2-phenylindole; DMEM, Dulbecco's minimal essential medium; ECL, Enhanced chemiluminescent; ELISA, Enzyme-linked immunosorbent assay; EGFR, Epidermal growth factor receptor; FBS, Fetal bovine serum; GFP, Green fluorescent protein; GSDM, Gasdermin; H&E, Hematoxylin and eosin; H/R, Hypoxia/reoxygenation; HCC, Hepatocellular carcinoma; HMGB1, High mobility group box 1; I/R, Ischemia/reperfusion; IEC-6, Intestinal epithelial cells-6; IL-18, Interleukin-18; IL-1α, Interleukin-1alpha; IL-1β, Interleukin-1beta; LDH, Lactate dehydrogenase; MODS, Multiple organ dysfunction syndromes;

NLRP3, NOD-, LRR-, and pyrin domain-containing 3; OD, Optical density; PBS, Phosphate-buffered saline; PI, Propidium iodide; PVDF, Polyvinylidene fluoride; ROS, Reactive oxygen species; SD, Standard deviation; SDS-PAGE, Sodium dodecyl sulfate polyacrylamide gel electrophoresis; SIRS, Systemic inflammatory response syndrome; SMA, Superior mesenteric artery; TNF-α, Tumor necrosis factor-α

Declarations

Funding

This study was supported by the Natural Science Foundation of Liaoning Province (No. 2019-MS-084).

Competing interests

The authors declare that there are no conflicts of interest in the present work.

Consent to participate

Not applicable

Consent for publication

All authors agree to publish the manuscript

Availability of data and material

Not applicable

Code availability

Not applicable

Authors' Contribution

F.W., D.S., L.G., and Y.W. performed experiments; F.W., Y.Z., L.X., and L.Y. performed data analysis; F.W., X.L., and Q.M. wrote main manuscript text; F.W., J.P., Y.L., and P.S. reviewed and edited manuscript; P.S. guided research.

References

1. Aizawa, E., T. Karasawa, S. Watanabe, T. Komada, H. Kimura, R. Kamata, H. Ito, E. Hishida, N. Yamada, T. Kasahara, Y. Mori and M. Takahashi (2020). "GSDME-Dependent Incomplete Pyroptosis Permits Selective IL-1alpha Release under Caspase-1 Inhibition." iScience **23**(5): 101070.
2. Arkhipov, A., Y. Shan, E. T. Kim and D. E. Shaw (2014). "Membrane interaction of bound ligands contributes to the negative binding cooperativity of the EGF receptor." PLoS Comput Biol **10**(7): e1003742.

3. Ayuso-Sacido, A., J. A. Moliterno, S. Kratovac, G. S. Kapoor, D. M. O'Rourke, E. C. Holland, J. M. Garcia-Verdugo, N. S. Roy and J. A. Boockvar (2010). "Activated EGFR signaling increases proliferation, survival, and migration and blocks neuronal differentiation in post-natal neural stem cells." J Neurooncol **97**(3): 323–337.
4. Basiorka, A. A., K. L. McGraw, E. A. Eksioglu, X. Chen, J. Johnson, L. Zhang, Q. Zhang, B. A. Irvine, T. Cluzeau, D. A. Sallman, E. Padron, R. Komrokji, L. Sokol, R. C. Coll, A. A. Robertson, M. A. Cooper, J. L. Cleveland, L. A. O'Neill, S. Wei and A. F. List (2016). "The NLRP3 inflammasome functions as a driver of the myelodysplastic syndrome phenotype." Blood **128**(25): 2960–2975.
5. Bertheloot, D., E. Latz and B. S. Franklin (2021). "Necroptosis, pyroptosis and apoptosis: an intricate game of cell death." Cell Mol Immunol **18**(5): 1106–1121.
6. Broz, P., P. Pelegrin and F. Shao (2020). "The gasdermins, a protein family executing cell death and inflammation." Nat Rev Immunol **20**(3): 143–157.
7. Chen, J., M. Wang, P. Zhang, H. Li, K. Qu, R. Xu, N. Guo and H. Zhu (2022). "Cordycepin alleviated metabolic inflammation in Western diet-fed mice by targeting intestinal barrier integrity and intestinal flora." Pharmacol Res **178**: 106191.
8. Chen, Q., P. Shi, Y. Wang, D. Zou, X. Wu, D. Wang, Q. Hu, Y. Zou, Z. Huang, J. Ren, Z. Lin and X. Gao (2019). "GSDMB promotes non-canonical pyroptosis by enhancing caspase-4 activity." J Mol Cell Biol **11**(6): 496–508.
9. Chen, Z., A. Mohr, B. Heitplatz, U. Hansen, A. Pascher, J. G. Brockmann and F. Becker (2020). "Sulforaphane Elicits Protective Effects in Intestinal Ischemia Reperfusion Injury." Int J Mol Sci **21**(15).
10. Coll, R. C., C. L. Holley and K. Schroder (2018). "Mitochondrial DNA synthesis fuels NLRP3 activation." Cell Res **28**(11): 1046–1047.
11. Dai, Y., Z. Mao, X. Han, Y. Xu, L. Xu, L. Yin, Y. Qi and J. Peng (2019). "MicroRNA-29b-3p reduces intestinal ischaemia/reperfusion injury via targeting of TNF receptor-associated factor 3." Br J Pharmacol **176**(17): 3264–3278.
12. Deitch, E. A. (1992). "Multiple organ failure. Pathophysiology and potential future therapy." Ann Surg **216**(2): 117–134.
13. Duranti, S., V. Vivo, I. Zini, C. Milani, M. Mangifesta, R. Anzalone, L. Mancabelli, A. Viappiani, A. M. Cantoni, E. Barocelli, D. van Sinderen, S. Bertoni and F. Turroni (2018). "Bifidobacterium bifidum PRL2010 alleviates intestinal ischemia/reperfusion injury." PLoS One **13**(8): e0202670.
14. El-Ahwany, E. G. E., L. Mourad, M. M. K. Zoheiry, H. Abu-Taleb, M. Hassan, R. Atta, M. Hassanien and S. Zada (2019). "MicroRNA-122a as a non-invasive biomarker for HCV genotype 4-related hepatocellular carcinoma in Egyptian patients." Arch Med Sci **15**(6): 1454–1461.
15. Eryilmaz, S., Z. Turkyilmaz, R. Karabulut, M. A. Gulburun, A. Poyraz, O. Gulbahar, B. Arslan and K. Sonmez (2020). "The effects of hydrogen-rich saline solution on intestinal anastomosis performed after intestinal ischemia reperfusion injury." J Pediatr Surg **55**(8): 1574–1578.

16. Feng, D., J. Yao, G. Wang, Z. Li, G. Zu, Y. Li, F. Luo, S. Ning, W. Qasim, Z. Chen and X. Tian (2017). "Inhibition of p66Shc-mediated mitochondrial apoptosis via targeting prolyl-isomerase Pin1 attenuates intestinal ischemia/reperfusion injury in rats." Clin Sci (Lond) **131**(8): 759–773.
17. Fernandez, A. R., R. Sanchez-Tarjuelo, P. Cravedi, J. Ochando and M. Lopez-Hoyos (2020). "Review: Ischemia Reperfusion Injury-A Translational Perspective in Organ Transplantation." Int J Mol Sci **21**(22).
18. Frank, D. and J. E. Vince (2019). "Pyroptosis versus necroptosis: similarities, differences, and crosstalk." Cell Death Differ **26**(1): 99–114.
19. Gonzalez, L. M., A. J. Moeser and A. T. Blikslager (2015). "Animal models of ischemia-reperfusion-induced intestinal injury: progress and promise for translational research." Am J Physiol Gastrointest Liver Physiol **308**(2): G63-75.
20. Gramantieri, L., M. Ferracin, F. Fornari, A. Veronese, S. Sabbioni, C. G. Liu, G. A. Calin, C. Giovannini, E. Ferrazzi, G. L. Grazi, C. M. Croce, L. Bolondi and M. Negrini (2007). "Cyclin G1 is a target of miR-122a, a microRNA frequently down-regulated in human hepatocellular carcinoma." Cancer Res **67**(13): 6092–6099.
21. He, W. T., H. Wan, L. Hu, P. Chen, X. Wang, Z. Huang, Z. H. Yang, C. Q. Zhong and J. Han (2015). "Gasdermin D is an executor of pyroptosis and required for interleukin-1beta secretion." Cell Res **25**(12): 1285–1298.
22. He, X., Y. Zheng, S. Liu, S. Shi, Y. Liu, Y. He, C. Zhang and X. Zhou (2018). "MiR-146a protects small intestine against ischemia/reperfusion injury by down-regulating TLR4/TRAF6/NF-kappaB pathway." J Cell Physiol **233**(3): 2476–2488.
23. Hu, Y., Z. Mao, L. Xu, L. Yin, X. Tao, Z. Tang, Y. Qi, P. Sun and J. Peng (2018). "Protective effect of dioscin against intestinal ischemia/reperfusion injury via adjusting miR-351-5p-mediated oxidative stress." Pharmacol Res **137**: 56–63.
24. Huang, X., Z. Feng, Y. Jiang, J. Li, Q. Xiang, S. Guo, C. Yang, L. Fei, G. Guo, L. Zheng, Y. Wu and Y. Chen (2019). "VSIG4 mediates transcriptional inhibition of Nlrp3 and Il-1beta in macrophages." Sci Adv **5**(1): eaau7426.
25. Itai, S., S. Yamada, M. K. Kaneko, Y. W. Chang, H. Harada and Y. Kato (2017). "Establishment of EMab-134, a Sensitive and Specific Anti-Epidermal Growth Factor Receptor Monoclonal Antibody for Detecting Squamous Cell Carcinoma Cells of the Oral Cavity." Monoclon Antib Immunodiagn Immunother **36**(6): 272–281.
26. Jia, C., J. Zhang, H. Chen, Y. Zhuge, H. Chen, F. Qian, K. Zhou, C. Niu, F. Wang, H. Qiu, Z. Wang, J. Xiao, X. Rong and M. Chu (2019). "Endothelial cell pyroptosis plays an important role in Kawasaki disease via HMGB1/RAGE/cathespin B signaling pathway and NLRP3 inflammasome activation." Cell Death Dis **10**(10): 778.
27. Jia, Y., R. Cui, C. Wang, Y. Feng, Z. Li, Y. Tong, K. Qu, C. Liu and J. Zhang (2020). "Metformin protects against intestinal ischemia-reperfusion injury and cell pyroptosis via TXNIP-NLRP3-GSDMD pathway." Redox Biol **32**: 101534.

28. Kip, A. M., J. Grootjans, M. Manca, M. Hadfoune, B. Boonen, J. P. M. Derikx, E. A. L. Biessen, S. W. M. Olde Damink, C. H. C. Dejong, W. A. Buurman and K. Lenaerts (2021). "Temporal Transcript Profiling Identifies a Role for Unfolded Protein Stress in Human Gut Ischemia-Reperfusion Injury." Cell Mol Gastroenterol Hepatol **13**(3): 681–694.
29. Kovacs, S. B. and E. A. Miao (2017). "Gasdermins: Effectors of Pyroptosis." Trends Cell Biol **27**(9): 673–684.
30. Latz, E., T. S. Xiao and A. Stutz (2013). "Activation and regulation of the inflammasomes." Nat Rev Immunol **13**(6): 397–411.
31. Lee, Y., C. Ahn, J. Han, H. Choi, J. Kim, J. Yim, J. Lee, P. Provost, O. Radmark, S. Kim and V. N. Kim (2003). "The nuclear RNase III Drosha initiates microRNA processing." Nature **425**(6956): 415–419.
32. Li, H. J., Y. B. Pan, Z. L. Sun, Y. Y. Sun, X. T. Yang and D. F. Feng (2018). "Inhibition of miR-21 ameliorates excessive astrocyte activation and promotes axon regeneration following optic nerve crush." Neuropharmacology **137**: 33–49.
33. Li, Q., B. Hu, G. W. Hu, C. Y. Chen, X. Niu, J. Liu, S. M. Zhou, C. Q. Zhang, Y. Wang and Z. F. Deng (2016). "tRNA-Derived Small Non-Coding RNAs in Response to Ischemia Inhibit Angiogenesis." Sci Rep **6**: 20850.
34. Li, Y., Y. Luo, B. Li, L. Niu, J. Liu and X. Duan (2020). "miRNA-182/Deptor/mTOR axis regulates autophagy to reduce intestinal ischaemia/reperfusion injury." J Cell Mol Med **24**(14): 7873–7883.
35. Li, Y., S. Wen, X. Yao, W. Liu, J. Shen, W. Deng, J. Tang, C. Li and K. Liu (2017). "MicroRNA-378 protects against intestinal ischemia/reperfusion injury via a mechanism involving the inhibition of intestinal mucosal cell apoptosis." Cell Death Dis **8**(10): e3127.
36. Li, Y., B. Xu, M. Xu, D. Chen, Y. Xiong, M. Lian, Y. Sun, Z. Tang, L. Wang, C. Jiang and Y. Lin (2017). "6-Gingerol protects intestinal barrier from ischemia/reperfusion-induced damage via inhibition of p38 MAPK to NF-kappaB signalling." Pharmacol Res **119**: 137–148.
37. Li, Z., G. Wang, D. Feng, G. Zu, Y. Li, X. Shi, Y. Zhao, H. Jing, S. Ning, W. Le, J. Yao and X. Tian (2018). "Targeting the miR-665-3p-ATG4B-autophagy axis relieves inflammation and apoptosis in intestinal ischemia/reperfusion." Cell Death Dis **9**(5): 483.
38. Lillo-Moya, J., C. Rojas-Sole, D. Munoz-Salamanca, E. Panieri, L. Saso and R. Rodrigo (2021). "Targeting Ferroptosis against Ischemia/Reperfusion Cardiac Injury." Antioxidants (Basel) **10**(5).
39. Liu, D. Q., S. P. Chen, J. Sun, X. M. Wang, N. Chen, Y. Q. Zhou, Y. K. Tian and D. W. Ye (2019). "Berberine protects against ischemia-reperfusion injury: A review of evidence from animal models and clinical studies." Pharmacol Res **148**: 104385.
40. Liu, L., J. Yao, Z. Li, G. Zu, D. Feng, Y. Li, W. Qasim, S. Zhang, T. Li, H. Zeng and X. Tian (2018). "miR-381-3p knockdown improves intestinal epithelial proliferation and barrier function after intestinal ischemia/reperfusion injury by targeting nurr1." Cell Death Dis **9**(3): 411.
41. Liu, Z., J. Jiang, Q. Yang, Y. Xiong, D. Zou, C. Yang, J. Xu and H. Zhan (2016). "MicroRNA-682-mediated downregulation of PTEN in intestinal epithelial cells ameliorates intestinal ischemia-reperfusion injury." Cell Death Dis **7**: e2210.

42. Matsuda, A., W. L. Yang, A. Jacob, M. Aziz, S. Matsuo, T. Matsutani, E. Uchida and P. Wang (2014). "FK866, a visfatin inhibitor, protects against acute lung injury after intestinal ischemia-reperfusion in mice via NF-kappaB pathway." Ann Surg **259**(5): 1007–1017.
43. Mendell, J. T. and E. N. Olson (2012). "MicroRNAs in stress signaling and human disease." Cell **148**(6): 1172–1187.
44. Merlino, G. T. (1990). "Epidermal growth factor receptor regulation and function." Semin Cancer Biol **1**(4): 277–284.
45. Nirmala, J. G. and M. Lopus (2020). "Cell death mechanisms in eukaryotes." Cell Biology and Toxicology **36**(2): 145–164.
46. Ohno, S., M. Takanashi, K. Sudo, S. Ueda, A. Ishikawa, N. Matsuyama, K. Fujita, T. Mizutani, T. Ohgi, T. Ochiya, N. Gotoh and M. Kuroda (2013). "Systemically injected exosomes targeted to EGFR deliver antitumor microRNA to breast cancer cells." Mol Ther **21**(1): 185–191.
47. Pan, D. S., P. Cao, J. J. Li, D. Fan and Z. Q. Song (2019). "MicroRNA-374b inhibits migration and invasion of glioma cells by targeting EGFR." Eur Rev Med Pharmacol Sci **23**(10): 4254–4263.
48. Pan, L. L., W. Liang, Z. Ren, C. Li, Y. Chen, W. Niu, X. Fang, Y. Liu, M. Zhang, J. Diana, B. Agerberth and J. Sun (2020). "Cathelicidin-related antimicrobial peptide protects against ischaemia reperfusion-induced acute kidney injury in mice." Br J Pharmacol **177**(12): 2726–2742.
49. Paul, S., L. A. Bravo Vazquez, S. Perez Uribe, P. Roxana Reyes-Perez and A. Sharma (2020). "Current Status of microRNA-Based Therapeutic Approaches in Neurodegenerative Disorders." Cells **9**(7).
50. Puleo, F., M. Arvanitakis, A. Van Gossum and J. C. Preiser (2011). "Gut failure in the ICU." Semin Respir Crit Care Med **32**(5): 626–638.
51. Purba, E. R., E. I. Saita and I. N. Maruyama (2017). "Activation of the EGF Receptor by Ligand Binding and Oncogenic Mutations: The "Rotation Model"." Cells **6**(2).
52. Qasim, W., Y. Li, R. M. Sun, D. C. Feng, Z. Y. Wang, D. S. Liu, J. H. Yao and X. F. Tian (2020). "PTEN-induced kinase 1-induced dynamin-related protein 1 Ser637 phosphorylation reduces mitochondrial fission and protects against intestinal ischemia reperfusion injury." World J Gastroenterol **26**(15): 1758–1774.
53. Rathinam, V. A., S. K. Vanaja and K. A. Fitzgerald (2012). "Regulation of inflammasome signaling." Nat Immunol **13**(4): 333–342.
54. Reifegerste, D., F. Czerwinski, M. Rosset, E. Baumann, E. Kludt and S. Weg-Remers (2019). "Demographic and cancer-related differences between self-seeking patients and supported patients: Analysis of cancer information-service data." Psychooncology **28**(4): 759–766.
55. Rutgeerts, P., W. J. Sandborn, B. G. Feagan, W. Reinisch, A. Olson, J. Johanns, S. Travers, D. Rachmilewitz, S. B. Hanauer, G. R. Lichtenstein, W. J. de Villiers, D. Present, B. E. Sands and J. F. Colombel (2005). "Infliximab for induction and maintenance therapy for ulcerative colitis." N Engl J Med **353**(23): 2462–2476.
56. Sasada, T., K. Azuma, J. Ohtake and Y. Fujimoto (2016). "Immune Responses to Epidermal Growth Factor Receptor (EGFR) and Their Application for Cancer Treatment." Front Pharmacol **7**: 405.

57. Shen, X., H. Wang, C. Weng, H. Jiang and J. Chen (2021). "Caspase 3/GSDME-dependent pyroptosis contributes to chemotherapy drug-induced nephrotoxicity." Cell Death Dis **12**(2): 186.
58. Shen, Z. Y., J. Zhang, H. L. Song and W. P. Zheng (2013). "Bone-marrow mesenchymal stem cells reduce rat intestinal ischemia-reperfusion injury, ZO-1 downregulation and tight junction disruption via a TNF-alpha-regulated mechanism." World J Gastroenterol **19**(23): 3583–3595.
59. Shi, J., W. Gao and F. Shao (2017). "Pyroptosis: Gasdermin-Mediated Programmed Necrotic Cell Death." Trends Biochem Sci **42**(4): 245–254.
60. Shoup, T. (2018). "As Low as Reasonably Practicable: An Approach to Managing Device Risk." Biomed Instrum Technol **52**(3): 248.
61. Song, H., C. Zhao, Z. Yu, Q. Li, R. Yan, Y. Qin, M. Jia and W. Zhao (2020). "UAF1 deubiquitinase complexes facilitate NLRP3 inflammasome activation by promoting NLRP3 expression." Nat Commun **11**(1): 6042.
62. Stein, R., F. Kapplusch, M. C. Heymann, S. Russ, W. Staroske, C. M. Hedrich, A. Rosen-Wolff and S. R. Hofmann (2016). "Enzymatically Inactive Procaspase 1 stabilizes the ASC Pyroptosome and Supports Pyroptosome Spreading during Cell Division." J Biol Chem **291**(35): 18419–18429.
63. Tu, W. L., L. R. You, A. P. Tsou and C. M. Chen (2018). "Pten Haplodeficiency Accelerates Liver Tumor Growth in miR-122a-Null Mice via Expansion of Periportal Hepatocyte-Like Cells." Am J Pathol **188**(11): 2688–2702.
64. Van Opdenbosch, N. and M. Lamkanfi (2019). "Caspases in Cell Death, Inflammation, and Disease." Immunity **50**(6): 1352–1364.
65. Wang, G., J. Yao, Z. Li, G. Zu, D. Feng, W. Shan, Y. Li, Y. Hu, Y. Zhao and X. Tian (2016). "miR-34a-5p Inhibition Alleviates Intestinal Ischemia/Reperfusion-Induced Reactive Oxygen Species Accumulation and Apoptosis via Activation of SIRT1 Signaling." Antioxid Redox Signal **24**(17): 961–973.
66. Wang, X., L. Fan, H. Yin, Y. Zhou, X. Tang, X. Fei, H. Tang, J. Peng, X. Ren, Y. Xue, C. Zhu, J. Luo, Q. Jin and Q. Jin (2020). "Protective effect of Aster tataricus extract on NLRP3-mediated pyroptosis of bladder urothelial cells." J Cell Mol Med **24**(22): 13336–13345.
67. Wang, X., E. K. Lam, J. Zhang, H. Jin and J. J. Sung (2009). "MicroRNA-122a functions as a novel tumor suppressor downstream of adenomatous polyposis coli in gastrointestinal cancers." Biochem Biophys Res Commun **387**(2): 376–380.
68. Wang, Y., H. Li, C. Xue, H. Chen, Y. Xue, F. Zhao, M. X. Zhu and Z. Cao (2021). "TRPV3 enhances skin keratinocyte proliferation through EGFR-dependent signaling pathways." Cell Biol Toxicol **37**(2): 313–330.
69. Wang, Y., X. Zhou, K. Zou, G. Chen, L. Huang, F. Yang, W. Pan, H. Xu, Z. Xu, H. Chen, J. Chen, S. Gong, X. Zhou, W. Xu and J. Zhao (2021). "Monocarboxylate Transporter 4 Triggered Cell Pyroptosis to Aggravate Intestinal Inflammation in Inflammatory Bowel Disease." Front Immunol **12**: 644862.
70. Wang, Z. (2017). "ErbB Receptors and Cancer." Methods Mol Biol **1652**: 3–35.
71. Wu, J., S. Lin, B. Wan, B. Velani and Y. Zhu (2019). "Pyroptosis in Liver Disease: New Insights into Disease Mechanisms." Aging Dis **10**(5): 1094–1108.

72. Xue, F., C. Yang, K. Yun, C. Jiang, R. Cai, M. Liang, Q. Wang, W. Bian, H. Zhou, Z. Liu and L. Zhu (2021). "RETRACTED ARTICLE: Reduced LINC00467 elevates microRNA-125a-3p to suppress cisplatin resistance in non-small cell lung cancer through inhibiting sirtuin 6 and inactivating the ERK1/2 signaling pathway." Cell Biol Toxicol.
73. Yang, L., Y. Guo, X. Fan, Y. Chen, B. Yang, K. X. Liu and J. Zhou (2020). "Amelioration of Coagulation Disorders and Inflammation by Hydrogen-Rich Solution Reduces Intestinal Ischemia/Reperfusion Injury in Rats through NF-kappaB/NLRP3 Pathway." Mediators Inflamm **2020**: 4359305.
74. Yang, Y., B. Gong, Z. Z. Wu, P. Shuai, D. F. Li, L. L. Liu and M. Yu (2019). "Inhibition of microRNA-129-5p expression ameliorates ultraviolet ray-induced corneal epithelial cell injury via upregulation of EGFR." J Cell Physiol **234**(7): 11692–11707.
75. Ye, D., S. Guo, R. Al-Sadi and T. Y. Ma (2011). "MicroRNA regulation of intestinal epithelial tight junction permeability." Gastroenterology **141**(4): 1323–1333.
76. Zeng, C. Y., C. G. Li, J. X. Shu, L. H. Xu, D. Y. Ouyang, F. Y. Mai, Q. Z. Zeng, C. C. Zhang, R. M. Li and X. H. He (2019). "ATP induces caspase-3/gasdermin E-mediated pyroptosis in NLRP3 pathway-blocked murine macrophages." Apoptosis **24**(9–10): 703–717.
77. Zhang, B., Y. Tian, P. Jiang, Y. Jiang, C. Li, T. Liu, R. Zhou, N. Yang, X. Zhou and Z. Liu (2017). "MicroRNA-122a Regulates Zonulin by Targeting EGFR in Intestinal Epithelial Dysfunction." Cell Physiol Biochem **42**(2): 848–858.
78. Zhang, X., J. Wu, Q. Liu, X. Li, S. Li, J. Chen, Z. Hong, X. Wu, Y. Zhao and J. Ren (2020). "mtDNA-STING pathway promotes necroptosis-dependent enterocyte injury in intestinal ischemia reperfusion." Cell Death Dis **11**(12): 1050.
79. Zheng, L., X. Han, Y. Hu, X. Zhao, L. Yin, L. Xu, Y. Qi, Y. Xu, X. Han, K. Liu and J. Peng (2019). "Dioscin ameliorates intestinal ischemia/reperfusion injury via adjusting miR-351-5p/MAPK13-mediated inflammation and apoptosis." Pharmacol Res **139**: 431–439.
80. Zheng, Z., T. Wang, J. Chen, H. Qiu, C. Zhang, W. Liu, S. Qin, J. Tian and J. Guo (2021). "Inflammasome-Induced Osmotic Pressure and the Mechanical Mechanisms Underlying Astrocytic Swelling and Membrane Blebbing in Pyroptosis." Front Immunol **12**: 688674.
81. Zhu, J., E. Shimizu, X. Zhang, N. C. Partridge and L. Qin (2011). "EGFR signaling suppresses osteoblast differentiation and inhibits expression of master osteoblastic transcription factors Runx2 and Osterix." J Cell Biochem **112**(7): 1749–1760.
82. Zuo, L., L. Zhou, C. Wu, Y. Wang, Y. Li, R. Huang and S. Wu (2020). "Salmonella spvC Gene Inhibits Pyroptosis and Intestinal Inflammation to Aggravate Systemic Infection in Mice." Front Microbiol **11**: 562491.

Figures

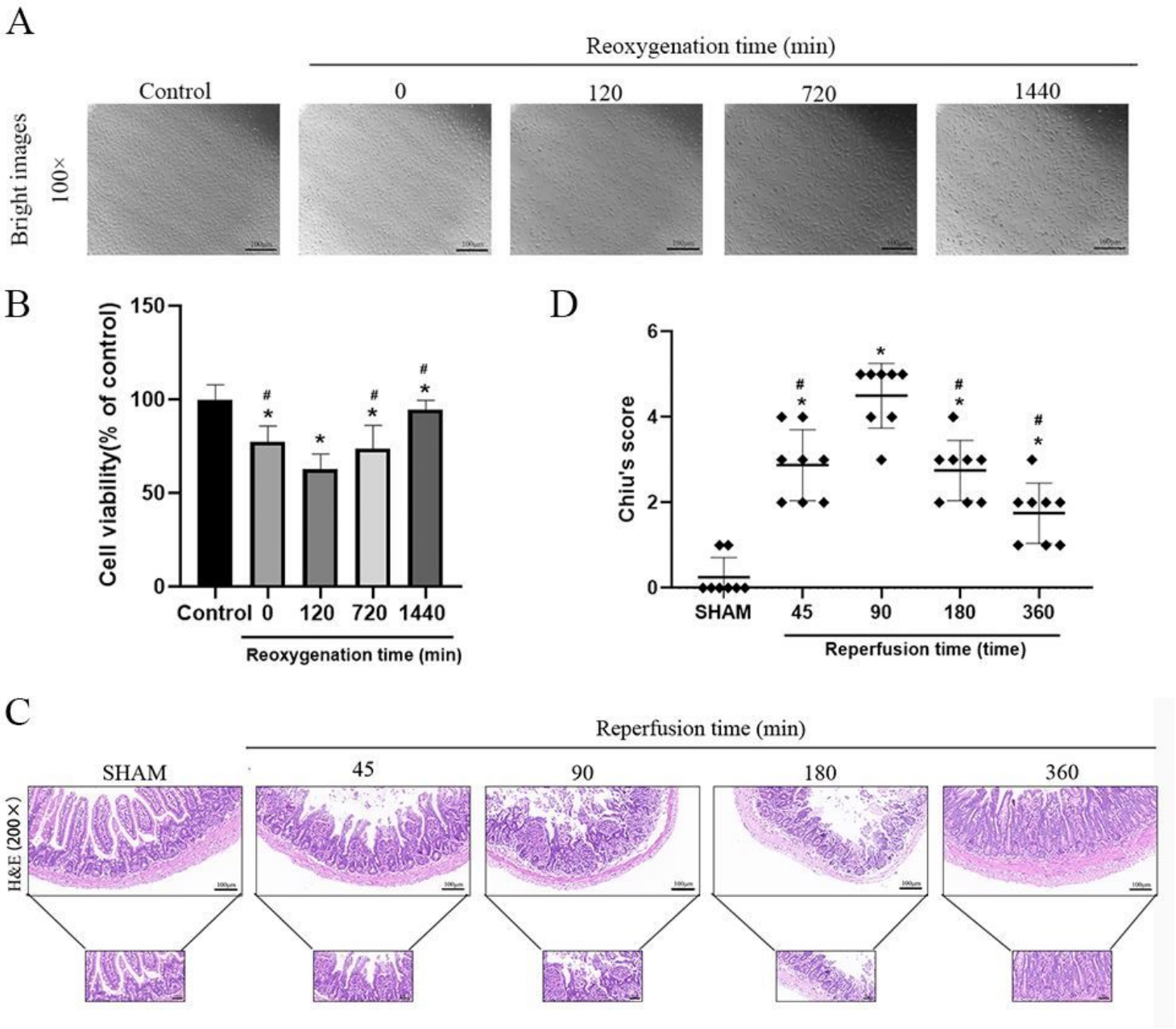

Figure 1

H/R- and I/R-induced cell and tissue injury. (A, B) IEC-6 cell viability and cellular morphology. Cell viability was evaluated using CCK-8 assay (n=6). H&E staining (C) and histopathological scores (D) in mice intestinal tissue (n=8). One sham group and four intestinal I/R groups (45 min of ischaemia followed by 45, 90, 180, or 360 min of reperfusion) were randomly assigned to mice. All data are presented as the mean±SD (n=5-8). $^{*}P<0.05$ shows a significant difference in comparison to the control groups or sham groups; $^{\#}P<0.05$ shows a significant difference in comparison to the 120 min of reoxygenation or 90 min of reperfusion groups.

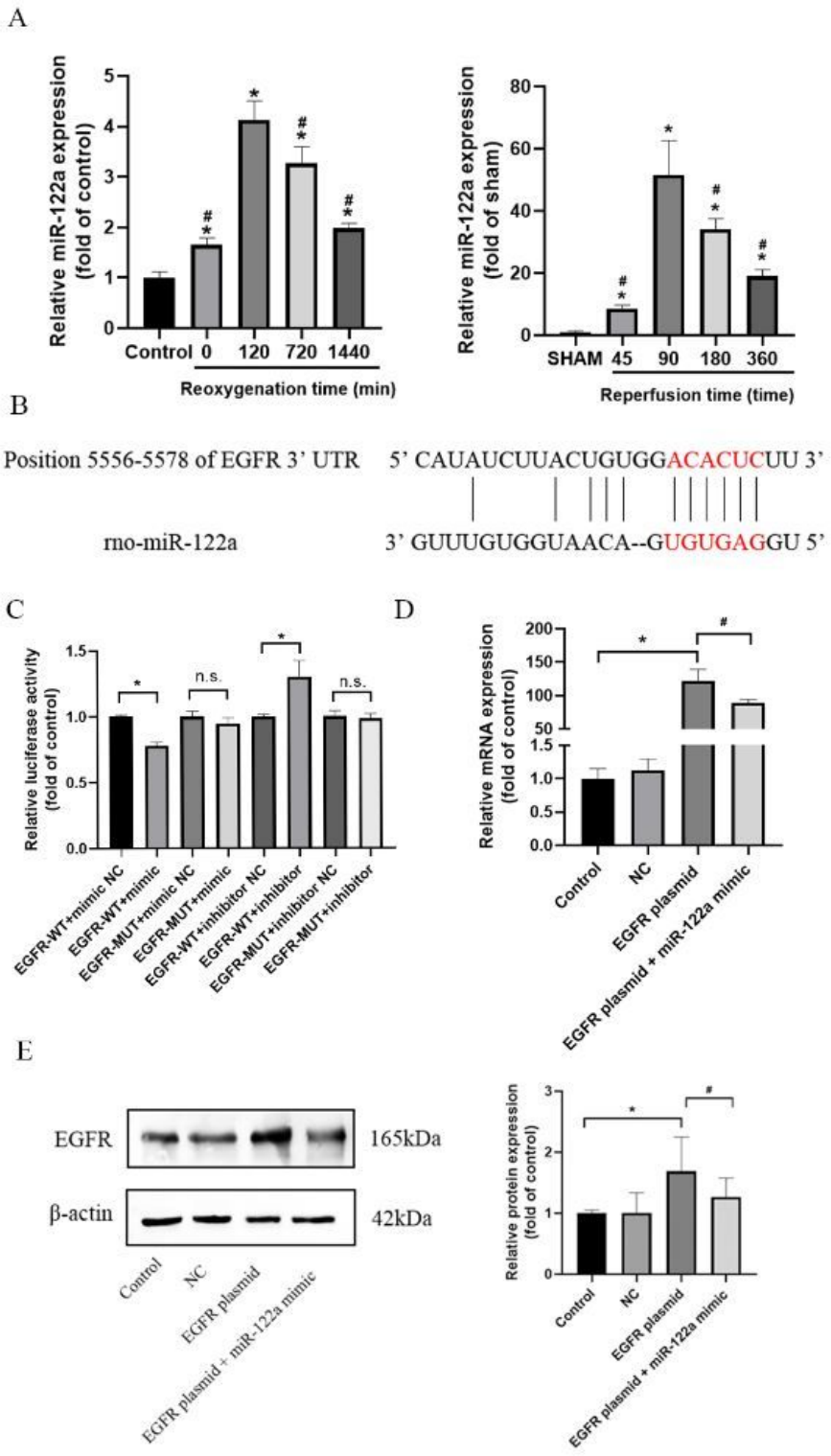

Figure 2

***In vitro* and *in vivo* experiments showed that EGFR was a target gene of miR-122a.** (A) miR-122a mRNA expression levels (qPCR) in H/R- and I/R-induced cell and intestinal injury. (B) A diagram showing miR-122a's conservative seed binding locations on target genes' 3'-UTRs (EGFR). (C) EGFR 3'-UTR relative luciferase expression after co-transfection with miR-122a mimic or NC (miR-122a inhibitor or NC). IEC-6 cells were co-transfected with miR-122a mimic or NC (miR-122a inhibitor or NC) and EGFR-WT or EGFR-

MUT in 24-well plates. The luciferase activities were measured using the Dual-Luciferase Reporter Assay Kit after 24 h of transfection. (D, E) Relative levels of EGFR expression following co-transfection. All data are presented as the mean±SD (n=5-6). *P<0.05 when contrasted to the control group in Figure 2A,D,E and the NC group in Figure 2C; #P<0.05 when contrasted to the 120 min of reoxygenation or 90 min of reperfusion group in Figure 2A and the EGFR-overexpression plasmid group in Figure 2D,E.

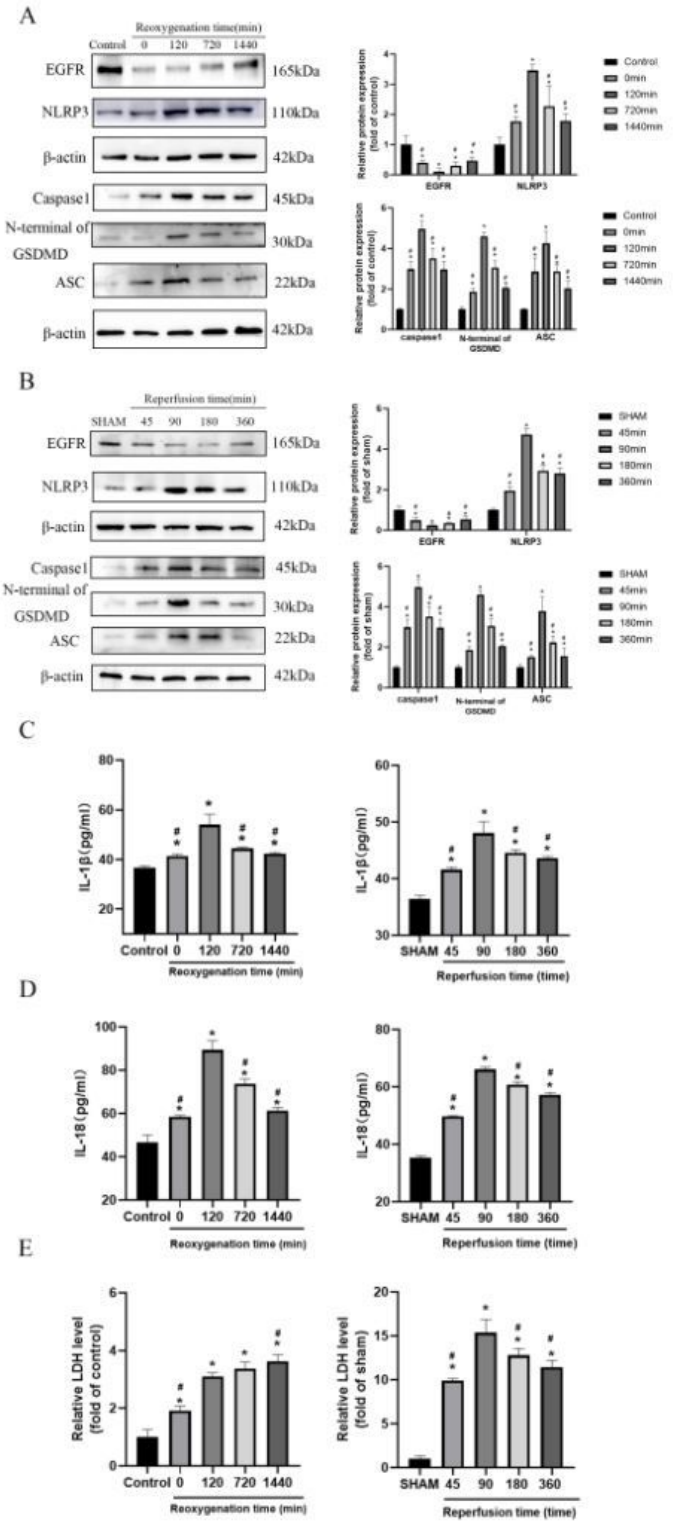

Figure 3

miR-122a adjusted EGFR signal pathway. EGFR, NLRP3, caspase 1, N-terminal GSDMD, and ASC protein levels measurement *in vitro* (A) and *in vivo* (B). Inflammatory factors IL-1β (C) and IL-18 (D) measurement *in vitro* and *in vivo*. (E) LDH release measurement. All data are presented as the mean±SD (n=5-6). *P<0.05 shows a significant difference in comparison to the control groups or sham groups; #P<0.05 shows a significant difference in comparison to the 120 min of reoxygenation or 90 min of reperfusion groups.

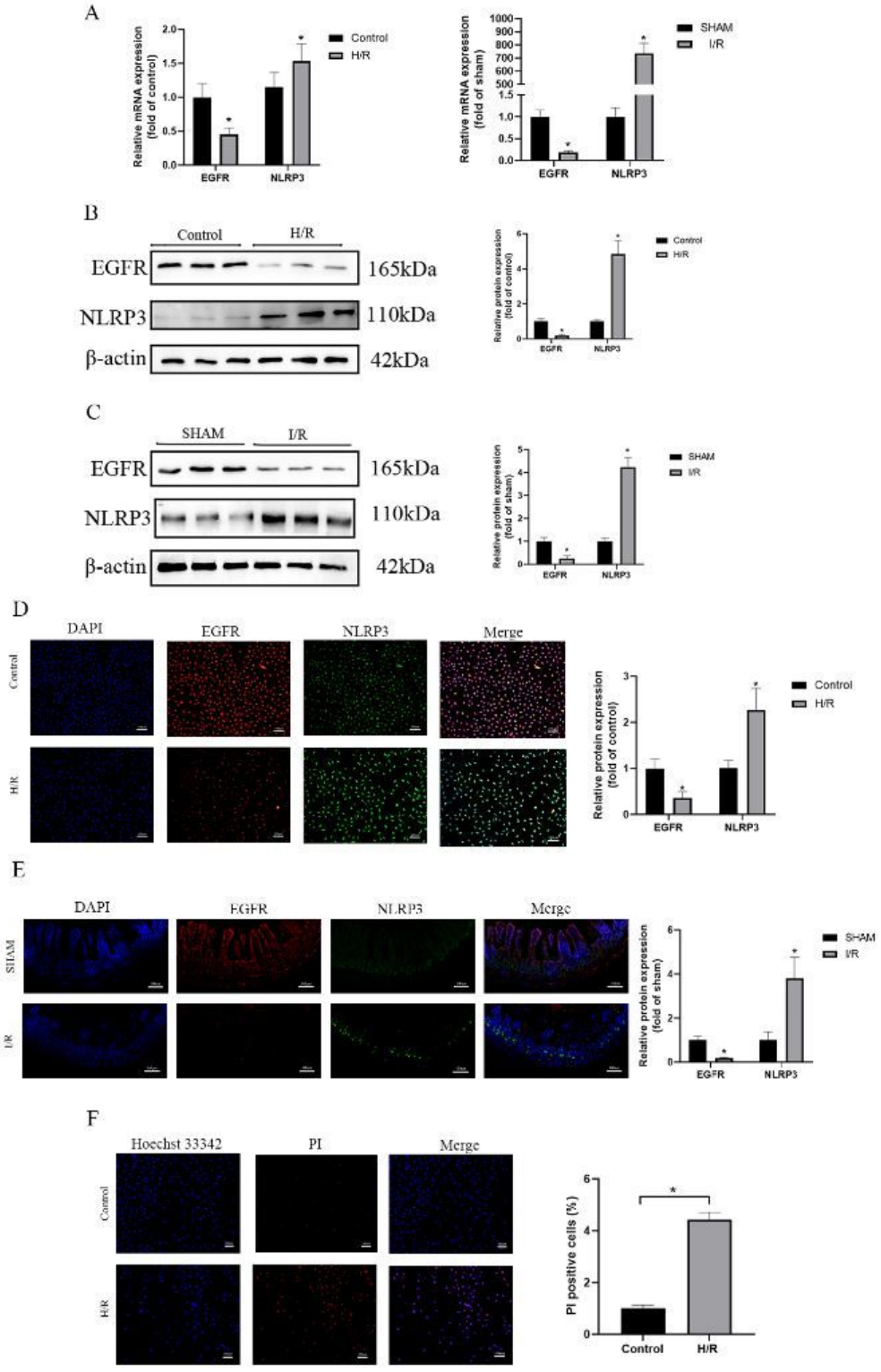

Figure 4

H/R- and I/R-induced intestinal inflammation and EGFR-NLRP3-related pyroptosis *in vitro* and *in vivo*. (A) qPCR assay on EGFR and NLRP3 mRNA expression levels following H/R- and I/R-induced injury. Western blotting assay on EGFR and NLRP3 protein expression levels following H/R- (B) and I/R-induced (C) injury. (D, E) Immunofluorescence assay on EGFR and NLRP3 protein expression levels following H/R- (D) and I/R-induced (E) injury. (F) Hoechst 33342 and PI staining assays on necrosis following H/R-induced IEC-6 cell injury. All data are presented as the mean±SD (n=5-6). $^{*}P<0.05$ shows a significant difference in comparison to the control groups or sham groups.

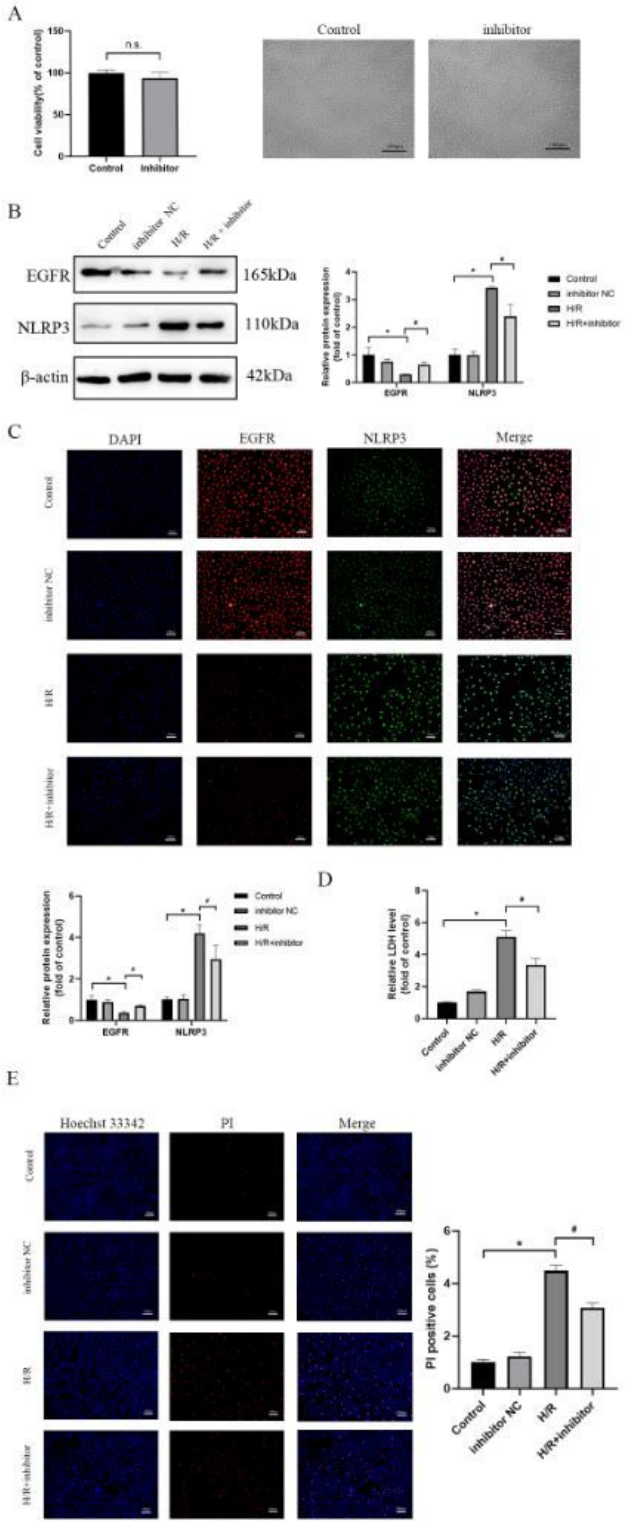

Figure 5

Inhibitor of miR-122a reduced H/R-induced injury *in vitro*. (A) IEC-6 cell viability and morphology following miR-122a inhibitor transfection. Western blotting (B) and immunofluorescence staining (C) assays on EGFR and NLRP3 protein expression levels following miR-122a inhibitor transfection. (D) LDH releasing measurement in IEC-6 cells. (E) Hoechst 33342 and PI staining assays on IEC-6 cell necrosis following miR-122a inhibitor transfection. All data are presented as the mean±SD (n=5-6). *P<0.05 shows a

significant difference in comparison to the control groups; #P<0.05 shows a significant difference in comparison to the H/R group; n.s., not significant.

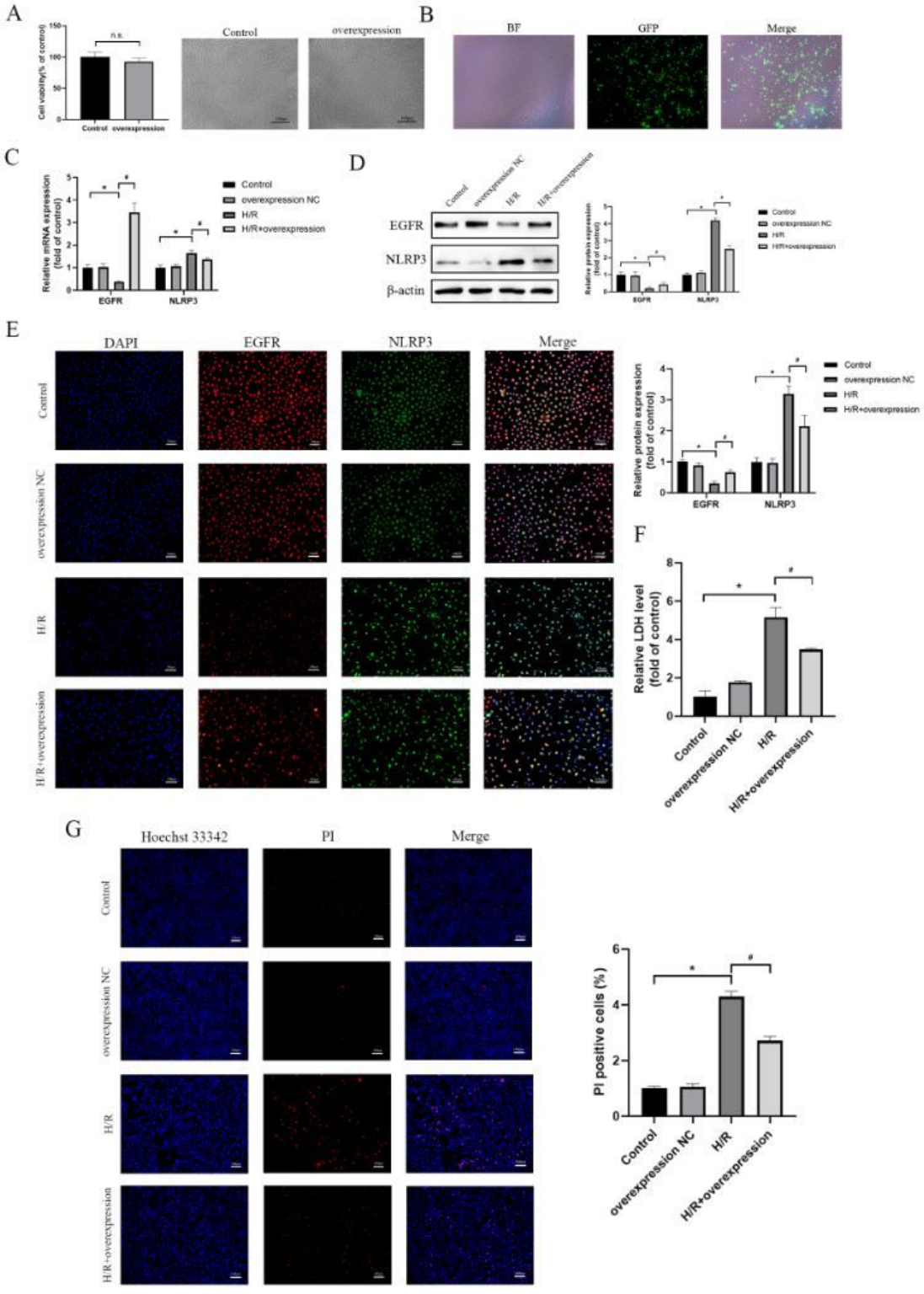

Figure 6

Overexpression of EGFR minimized H/R-induced injury in vitro. (A) IEC-6 cell viability and morphology following EGFR-overexpression transfection. (B) GFP fluorescence assay on transfection ratio of IEC-6

cells following EGFR-overexpression transfection. (C) qPCR assay on EGFR and NLRP3 mRNA expression levels after H/R injury and H/R injury following EGFR-overexpression transfection. Western blotting (D) and immunofluorescence staining (E) assays on EGFR and NLRP3 protein expression levels following EGFR-overexpression transfection. (F) LDH releasing measurement in IEC-6 cells. (G) Hoechst 33342 and PI staining assays on IEC-6 cell necrosis following EGFR-overexpression transfection. All data are presented as the mean±SD (n=5-6). *P<0.05 shows a significant difference in comparison to the control groups; $^{\#}$P<0.05 shows a significant difference in comparison to the H/R group; n.s., not significant.

Supplementary Files

This is a list of supplementary files associated with this preprint. Click to download.

- GA.jpg
- SupplementaryTableS1.Thesequencesofprimers..docx